CHEMISTRY OF MATERIALS



Article

# Zwitterionic Poly(betaine-*N*-isopropylacrylamide) Microgels: Properties and Applications

Mallika Das, Nicolas Sanson, and Eugenia Kumacheva

*Chem. Mater.*, **2008**, 20 (22), 7157-7163 • Publication Date (Web): 29 October 2008



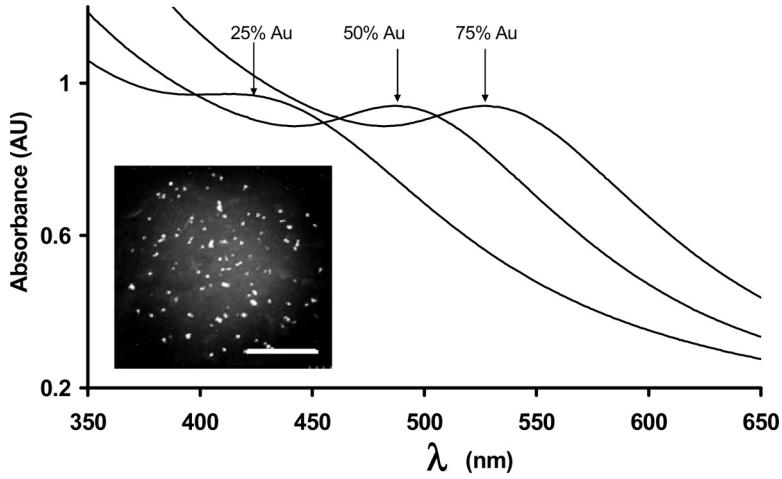


## More About This Article

Additional resources and features associated with this article are available within the HTML version:

- Supporting Information
- Access to high resolution figures
- Links to articles and content related to this article
- Copyright permission to reproduce figures and/or text from this article

View the Full Text HTML



Chemistry of Materials is published by the American Chemical Society. 1155 Sixteenth Street N.W., Washington, DC 20036

# Zwitterionic Poly(betaine-*N*-isopropylacrylamide) Microgels: Properties and Applications

Mallika Das, Nicolas Sanson, and Eugenia Kumacheva*

*Department of Chemistry, University of Toronto, 80 Saint George Street, Toronto, Ontario M5S 3H6, Canada*

*Received June 11, 2008. Revised Manuscript Received September 24, 2008*

We report the synthesis of zwitterionic poly(*N*,*N*-dimethyl-*N*-(3-methacrylamidopropyl)-*N*-(3-sulfopropyl) ammonium betaine-isopropylacrylamide) (poly(NIPAm-SPP)) microgels prepared by free-radical precipitation polymerization. We investigated the influence of the amount of SPP and the effect of the variations in temperature, pH, and electrolyte concentration on the microgel dimensions. In the range of the concentrations of SPP studied in the present work, no expected antipolyelectrolyte behavior of the microgels was observed and the particles showed polyelectrolyte properties. The zwitterionic properties of the microgels were used for in situ template-based synthesis of gold, silver, and bimetallic gold−silver nanoparticles.

## Introduction

Polyampholyte microgels (PAMs) carry both positive and negative charges in a broad range of physicochemical conditions.[1−5] These microgels exhibit rich phenomenology in their stimuli responsive properties, due to the complex interactions between the oppositely charged functional groups.[6] For example, PAMs show pH-dependent volume transitions which are determined by the relative numbers and types of ionized groups. Typically, the pH-induced variation in size of PAMs containing weak acidic and basic groups exhibits two peaks at low and high pH, which correspond to the maximum charge of the cationic and anionic groups, respectively.[4,7] In the intermediate pH range, the formation of ion couples between the oppositely charged groups leads to microgel deswelling.[8,9] In contrast, PAMs functionalized with strong acidic and basic groups are not pH-sensitive because they are charged in the entire pH range.[10]

Polyelectrolyte and polyampholyte microgels functionalized with strong or weak acidic or basic groups undergo volume transitions in salt solutions. Microgels with noncompensated positive or negative charges display polyelectrolyte behavior, which is characterized by deswelling, because of the screening of repulsion between oppositely charged groups by free ions. When charges of oppositely charged groups are compensated by ion coupling (that is, at near net-zero charge densities) PAMs exhibit antipolyelectrolyte behavior characterized by swelling at high salt concentrations, because of electrostatic screening of the opposite charges by the free ions.[11]

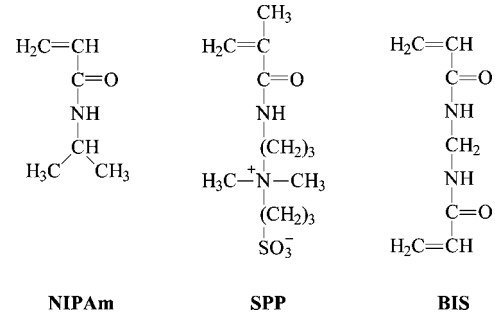


**Figure 1.** Chemical structure of monomers used in the syntesis of microgels: *N*-isopropylacrylamide (NIPAm); *N*,*N*-dimethyl-*N*-(3-methacrylamidopropyl)-*N*-(3-sulfopropyl) ammonium betaine (SPP); and*N*-*N*′-methylene-bisacrylamide (BIS).

Typically, PAMs are synthesized by precipitation copolymerization of cationic and anionic monomers.[3,9] The distribution of charged groups within the microgels is determined by the reactivity of comonomers and the solubility of the corresponding polymers. These two factors can lead to the formation of microgels with a uniform, a gradient, or a core−shell structure, each with characteristic swelling−deswelling profiles.[12] The structural differences cast ambiguity over the interpretation of the volume transitions in PAMs, because their swelling properties are largely governed by the interactions of oppositely charged groups that are in close proximity. This problem can be overcome by synthesizing PAMS from zwitterionic monomers, in order to introduce an equal number of charged cationic and anionic groups to the microgels.

Sulfobetaines are an important class of zwitterionic monomers that contain a quaternary ammonium and a

* Corresponding author. E-mail: ekumache@alchemy.chem.utoronto.ca.

(1) Baker, J. P.; Blanch, H. W.; Prausnitz, J. M. *Polymer* **1995**, *36*, 1061.
(2) Kudaibergenov, S. E.; Ciferri, A. *Macromol. Rapid Commun.* **2007**, *28*, 1969.
(3) Neyret, S.; Vincent, B. *Polymer* **1997**, *38*, 6129.
(4) Ogawa, K.; Nakayama, A.; Kokufuta, E. *Langmuir* **2003**, *19*, 3178.
(5) Kelly, K. L.; Coronado, E.; Zhao, L. L.; Schatz, G. C. *J. Phys. Chem. B* **2003**, *107*, 668.
(6) Nisato, G.; Munch, J. P.; Candau, S. J. *Langmuir* **1999**, *15*, 4236.
(7) Das, M.; Kumacheva, E. *Colloid Polym. Sci.* **2006**, *284*, 1073.
(8) Kim, J.; Nayak, S.; Lyon, L. A. *J. Am. Chem. Soc.* **2005**, *127*, 9588.
(9) Das, M.; Zhang, H.; Kumacheva, E. *Ann. Rev. Mater. Res.* **2006**, *36*, 117.
(10) Didukh, A. G.; Koizhaiganova, R. B.; Khamitzhanova, G.; Bimendina, L. A.; Kudaibergenov, S. E. *Polym. Intern.* **2003**, *52*, 883.
(11) Huglin, M. B.; Rego, J. M. *Macromolecules* **1993**, *26*, 3118.
(12) Hoare, T.; McLean, D. *J. Phys. Chem. B* **2006**, *110*, 20327.

10.1021/cm801585x CCC: $40.75 
Published on Web 10/29/2008

sulfonate group separated by methylene units.[13−16] The persistent charged state of the sulfonate and quarternary ammonium groups allows sulfobetaine-functionalized microgels to maintain a constant near net-zero charge irrespective of the pH of the medium. Although the properties of macroscopic polybetaine gels have been reported by several research groups[11,14,16−24] currently, no report describing the synthesis, properties, and applications of zwitterionic polybetaine-based microgels exists. In comparison with bulk hydrogels, such microgels would offer greater surface area conducive to ion-trapping and microreactor type applications.[9]

Here we report surfactant-free synthesis of zwitterionic, polybetaine-based microgels by free radical precipitation polymerization. We copolymerized *N*-isopropylacrylamide (NIPAm) and *N*,*N*′-Dimethyl-*N*-(3-methacrylamidopropyl)-*N*-(3-sulfopropyl) ammonium betaine (SPP) in various molar ratios to produce poly(NIPAm-SPP) microgels. Incorporation of SPP monomers carrying both cationic and anionic groups afforded microgels with equal number of oppositely charged groups. We examined the effect of microgel composition on the swelling transitions of poly(NIPAm-SPP) microgels in response to changes in temperature, pH, and electrolyte concentrations. Furthermore, we used the simultaneous presence of anionic and cationic groups in the zwitterionic polybetaine microgels for the template-based synthesis of gold, silver, and bimetallic gold−silver nanoparticles.

## Experimental Section

**Materials.** *N*-isopropylacrylamide (NIPAm), a cross-linking agent *N*,*N*′-methylene-bis-acrylamide (BIS), and an initiator potassium persulfate (KPS) were purchased from Aldrich Canada and used as received. *N*,*N*-dimethyl-*N*-(3-methacrylamidopropyl)-*N*-(3-sulfopropyl) ammonium betaine (SPP) was donated by RASCHIG Gmbh, Germany. The structures of monomers used in the synthesis of microgels are provided in Figure 1. Deionized water at 18.2 mΩ was obtained from a Millipore-Q setup.

**Synthesis of Zwitterionic Poly(NIPAm-SPP) Microgels.** Poly(NIPAm-SPP) microgels were prepared by surfactant-free free radical precipitation polymerization.[25] Typically, an aqueous solution (90 mL) containing comonomers was placed in a 250 mL jacketed round-bottom flask equipped with a nitrogen inlet. The solution was stirred at 300 rpm under nitrogen for 30 min, and then heated to 70 °C. Then, 9 mL of an aqueous solution of KPS was injected. The polymerization was carried out for 5 h at 70 °C. Following the synthesis, the system was purified by dialysis (Spectra-POR membrane, 8000 KD) for 1 week against deionized water with twice daily changes of water. Following the dialysis, purification was carried out by centrifugation at 18 000× G for 30 min at room temperature in a temperature-controlled centrifuge. The sample codes and the recipes used for the microgel synthesis are provided in Table 1. A polyNIPAm microgel (Sample NS0) was used as a control system.

**Table 1. Formulations Used in Microgel Synthesis and the Corresponding Hydrodynamic Diameters, $D_h$, of Microgel Particles[a]**

| | reaction mixture (g) | | | | | |
|---|---|---|---|---|---|---|
| sample | NIPAm | SPP | BIS | KPS | water | $D_h$ (nm) |
| NSO | 0.89 | 0 | 0.05 | 0.06 | 99 | 646 |
| NS1 | 0.87 | 0.04 | 0.05 | 0.05 | 99 | 682 |
| NS2 | 0.84 | 0.05 | 0.05 | 0.06 | 99 | 739 |
| NS3 | 0.83 | 0.06 | 0.05 | 0.06 | 99 | 817 |
| NS4 | 0.83 | 0.07 | 0.05 | 0.06 | 99 | 1213 |

[a] Microgel dimensions were measured by photon correlation spectroscopy in deionized water at 25 °C. The error associated with the measurements was ±3.7%.

**Characterization of Microgel Particles.** The mean hydrodynamic diameter, $D_h$, of the microgels was measured using photon correlation spectroscopy (Zetasizer 3000HS, Malvern, UK) with a 10 mW laser operating at 633 nm. These experiments were carried out at room temperature at the scattering angle of 90°. A CONTIN statistical method was used to convert the measured correlation data into a particle size distribution. The temperature-dependent variation of microgel size was determined in the temperature range from 15 to 60 °C using photon correlation spectroscopy (Protein Solutions Inc.) equipped with a temperature controller. At each temperature, prior to the measurements, microgel dispersions were stabilized for 20 min. The pH of the dispersions was adjusted by adding either HCl or NaOH solutions in microgel dispersions.

**Sequestration of Metal Ions.** To sequester metal ions in microgels, 100 μL of microgel dispersion were mixed with 3 mL of 0.1M. $AgNO_3$ solution (for sequestration of $Ag^+$ ions) or 4 mL of 25 mM $HAuCl_4$ (for sequestration of $AuCl_4^-$ ions) and stirred for 30 min at room temperature. The dispersion was then centrifuged at 18 000 G for 30 min. Microgel precipitate was redispersed in deionized water (Milli-Q, 18.2 mΩ).

**Synthesis of Metal Nanoparticles in the Interior of Microgels.** Gold and silver nanoparticles (NPs) were synthesized by sequestration of $AuCl_4^-$ or $Ag^+$ ions respectively, into microgels, removing excess free ions by centrifugation, and subsequent reduction of the ions entrapped in microgels using an ice-cold solution of freshly prepared $NaBH_4$. Twenty μL of 0.01 M $NaBH_4$ solution were added under constant stirring to 3 mL of the centrifuged microgel dispersion containing $Ag^+$ or $AuCl_4^-$ ions. Following the addition of $NaBH_4$ the dispersions containing $Ag^+$ ions turned from clear to a yellow color, while the dispersion containing $AuCl_4^-$ ions turned from clear to a pale pink color.

**Synthesis of Bimetallic Nanoparticles in the Interior of Microgels.** The synthesis of bimetallic NPs was carried out in two stages. In the first stage, either gold or silver NPs were synthesized in the microgels as described above. In one series of experiments, hybrid microgel dispersions containing gold NPs were centrifuged, redispersed in 4 mL of 0.1 M aqueous solution of $AgNO_3$ solution, and allowed to equilibrate overnight. This dispersion was centrifuged for 30 min at 10 000 G and redispersed in deionized water. Ten microliters of an ice-cold solution of freshly prepared 0.01 M $NaBH_4$ was added to this dispersion. The dispersion immediately change color from purple to a brown-gray color.

Alternatively, hybrid microgel dispersions containing silver NPs were centrifuged and redispersed in 4 mL of 0.025 M $HAuCl_4$ solution and allowed to equilibrate for 2 h under stirring. The addition of 10 μL of an ice-cold solution of freshly prepared 0.01 M $NaBH_4$ to this dispersion yielded an immediate change in color from yellow to intense purple.

(13) Lee, W. F.; Chen, C. F. *Polym. Gels Networks* **1998**, *6*, 493.
(14) Kabiri, K.; Faraji-Dana, S.; Zohuriaan-Mehr, M. J. *Polym. Adv. Technol.* **2005**, *16*, 659.
(15) Lee, W. F.; Yeh, P. L. *J. Appl. Polym. Sci.* **1999**, *74*, 2170.
(16) Xue, W.; Champ, S.; Huglin, M. B. *Eur. Polym. J.* **2001**, *37*, 869.
(17) Lee, W. F.; Chen, C. F. *J. Appl. Polym. Sci.* **1998**, *69*, 2021.
(18) Huglin, M. B.; Rego, J. M. *Colloid Polym. Sci.* **1992**, *270*, 234.
(19) Huglin, M. B.; Rego, J. M. *Macromolecules* **1991**, *24*, 2556–2563.
(20) Huglin, M. B.; Rego, J. M. *Polymer* **1991**, *32*, 3354.
(21) Xue, W.; Huglin; M, B.; Liao, B.; Jones, T. G. J. *Eur. Polym. J.* **2007**, *43*, 915.
(22) Xue, W.; Huglin; M, B.; Liao, B. *Eur. Polym. J.* **2007**, *43*, 4355.
(23) Xue, W.; Huglin, M. B.; Liao, B. *Eur. Polym. J.* **2006**, *42*, 3015.
(24) Lee, W. F.; Chiu, R. J. *J. Polym. Res., Taiwan* **2002**, *9*, 141.
(25) Pelton, R. *Adv. Colloid Interface Sci.* **2000**, *85*, 1.

In the second approach to the synthesis of bimetallic NPs the sequestration of ions by the microgels was carried out by dispersing 100 $\mu$L of polymer microgel dispersion in the solution of $AgNO_3$ and $HAuCl_4$ with varying compositions, while keeping the net ion concentration of the salts below 1.5 mM. Following centrifugation of the dispersion of ion-loaded microgels, the particles were redispersed in deionized water. During these experiments we maintained a reaction quotient below the solubility product, $K_{sp}$ of AgCl(s), $1.6 \times 10^{-10}$.[26]

Upon reduction of the metal ions, the color of the system varied with the molar fractions of $AgNO_3$ and $HAuCl_4$ used. Typically, it changed from orange to red with increasing as $AuCl_4^-/Ag^+$ molar ratio.

A Hitachi HD 2000 Scanning Transmission Electron Microscope was used for imaging of the hybrid microgels. Energy-dispersive X-ray spectroscopy (Oxford Instruments, Inca) was used for elemental analysis and mapping to detect and determine the presence, locations, and relative amounts of gold and silver NPs in the microgel interior.

## Results and Discussion

**Effect of SPP Concentration on Dimensions of Poly-(NIPAm-SPP) Microgels.** Table 1 shows that hydrodynamic diameters of poly(NIPAm-SPP) microgels increased with increasing concentration of SPP in the reaction mixture. In particular, the diameter of microgels of series NS4 was almost 100% larger than that of polyNIPAm microgels (series NS0). This effect was unexpected because of the formation of ionic complexes between the oppositely charged groups of SPP; the copolymerization of this monomer with NIPAm was expected to increase intraparticle attraction between the ionic groups and result in microgel shrinkage.[10,16,27] We ascribe an increase in particle size with increasing (but still small) fraction of the SPP comonomer to the higher net hydrophilicity of the polymer network, caused by the presence of ionized groups. When the concentration of SPP in the reaction mixture exceeded 0.07 g, the microgel particles aggregated. Therefore higher concentrations of SPP in the reaction mixture system were avoided.

**Effect of pH.** We examined the effect of pH on the swelling properties of poly(NIPAm-SPP) microgels in the range $3 \leq$ pH $\leq 10$. Figure 2 shows that regardless of the microgel composition, the hydrodynamic diameter, $D_h$, of particles did not notably change in the entire range of pH. This result was in striking difference with the appearance of the two swelling peaks at low and high pH, which were measured for PAMs functionalized with weak acid and weak base moieties.[3,9,10,28,29] In principle, the change in microgel size could be caused by two effects: deionization of charged groups and the formation of ion couples. We note that in the present work, the microgels retained their zwitterionic state in the entire pH range because of the strong ionization of

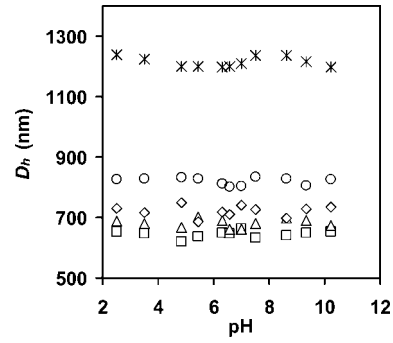


**Figure 2.** Variation in hydrodynamic diameters, $D_h$, plotted as a function of the value of pH for poly(NIPAm-SPP) microgels: (□) NS0; (Δ) NS1; (◇) NS2; (○) NS3; (∗) NS4. Error of measurements was estimated to be 15 ± 1%.

quaternary ammonium and sulfonate groups (for which the values of p$K_a$ in bulk are ~13.1 and ~ 0.7, respectively).[27,30]

In the whole pH range, the value of electrophoretic mobility of the poly(NIPAm-SPP) microgels did not exceed −0.264 $\mu$m cm/(V s), similar to the polyNIPAm microgels. The small negative charge of the microgels originated from the presence of the residues of anionic initiator potassium persulfate on the polymer chains. Therefore, we conclude that in the entire pH range ion pairing between the cationic and anionic groups did not occur.

**Effect of Temperature.** Figure 3a shows the variation of the mean hydrodynamic diameter of the poly(NIPAm-SPP) microgels as a function of temperature. For all zwitterionic microgels the volume phase transition temperatures (VPTTs) were in the range from 32 to 34 °C, that is, slightly higher than for the polyNIPAm microgels (Series NS0). In Figure 3b we plotted the change in hydrodynamic diameter $D_h/D_0$, where $D_0$ is the hydrodynamic diameter of microgels in the shrunken state at 50 °C. The zwitterionic microgels showed a substantially smaller degree of shrinkage which occurred in a broader temperature range than that for the polyNIPAm microgels. For example, between 29 and 45 °C, the microgels of the series NS2 and NS0 underwent 75 and 89% reduction in volume, respectively. This effect was counterintuitive: with increasing concentration of SPP, ion coupling was expected to result in larger deswelling of the zwitterionic microgels in water.

**Effect of Electrolytes.** We further studied the effect of electrolytes on the properties of poly(NIPAm-SPP) microgels by measuring the size of microgels in aqueous solutions of monovalent and divalent salts at different temperatures. Panels a and b in Figure 4 show the volume−temperature phase transitions of zwitterionic microgels (series NS3) dispersed in the solutions of KCl and $CdCl_2$, respectively.

In both systems, the microgels showed several similar trends. With salt concentration increasing from $1 \times 10^{-5}$ M to 1 M, the values of VPTT shifted to progressively lower values. No significant difference in microgel dimensions in the shrunken state (at 45 °C) was observed with increasing electrolyte concentration. The onset of microgel deswelling shifted to lower temperatures with increasing salt concentra-

(26) Mallin, M. P.; Murphy, C. J. *Nano Lett.* **2002**, *2*, 1235.
(27) Kudaibergenov, S.; Jaeger, W.; Laschewsky, A. Polymeric betaines: Synthesis, characterization, and application. In *Supramolecular Polymers/ Polymeric Betains/Oligomers*; Advances in Polumer Science Series; Springer: New York, 2006; Vol. 201, p 157.
(28) Kudaibergenov, S. E. *Phys. Chem. Chem. Phys.* **1996**, *100*, 1079.
(29) Tominaga, M.; Shimazoe, T.; Nagashima, M.; Taniguchi, I. *J. Electroanal. Chem.* **2008**, *615*, 51.
(30) Madura, J. D.; Lombardini, J. B.; Briggs, J. M.; Minor, D. L.; Wierzbicki, A. *Amino Acids* **1997**, *13*, 131.

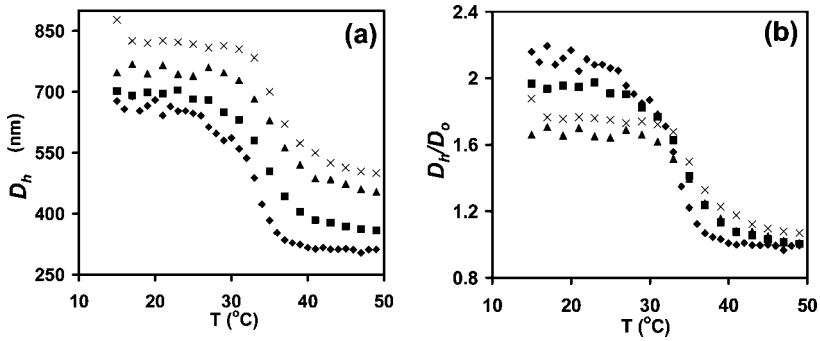


**Figure 3.** Variation in (a) hydrodynamic diameters $D_h$ and (b) normalized hydrodynamic diameters $D_h/D_0$ of the microgels, plotted as a function of temperature where $D_0$ is the mean hydrodynamic diameter of microgels at 50 °C. The particles were dispersed in water at pH 7. (♦) NS0; (□) NS1; (▲) NS2; (×) NS3. Error was estimated to be 15 ± 1%.

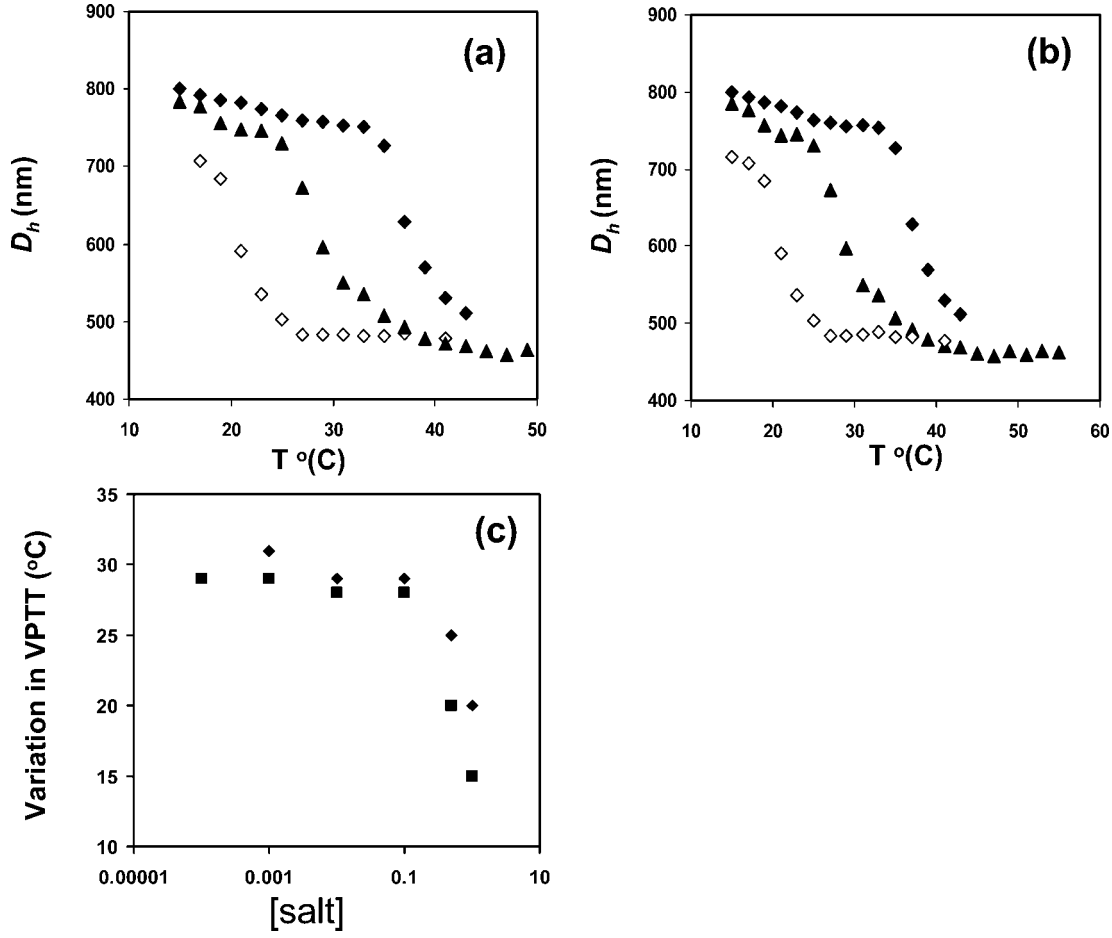


**Figure 4.** Effect of concentration of (a) KCl and (b) $CdCl_2$ on the temperature-induced variation in dimensions of poly(NIPAm-SPP) microgels of the series SN3. Salt concentration: $1 \times 10^{-5}$ M (♦); $5 \times 10^{-1}$ M (▲); and 1 M (◇). (c) Variation in onset of the VPTT plotted as a function of salt concentration. (♦) KCl (□) $CdCl_2$.

tion, as shown in Figure 4c. This decrease was gradual up to 0.1 M electrolyte concentration, but sharper at higher salt concentrations.

Figure 4 explicitly shows that no antipolyelectrolyte behavior was observed for the zwitterionic microgels in the presence of monovalent and divalent salts, similarly to trivalent salts (not shown). Instead, we observed a polyelectrolyte behavior: a decrease in microgel size and a lower VPTT with increasing salt concentration, more prominent with increasing content of the zwitterionic SPP in the microgels. These results are similar to previous reports on the polyelectrolyte behavior of macroscopic betaine poly-(NIPAm-SPP) hydrogels in solutions of monovalent salts[31] with concentrations in the range from $1 \times 10^{-5}$ to $1 \times 10^{-1}$ M.[15] However, in contrast to our work, an antipolyelectrolyte behavior was observed in the presence of divalent salts[31] and at high (above 1 M) salt concentrations.[15] Furthermore, unlike in our work, the total loss of temperature sensitivity of macroscopic gels was reported for high salt concentrations and it was ascribed to the increased solubility of SPP in salt solutions.[31]

(31) Cai, W.; Gupta, R. B. *J. Appl. Polym. Sci.* **2003**, *88*, 2032–2037.

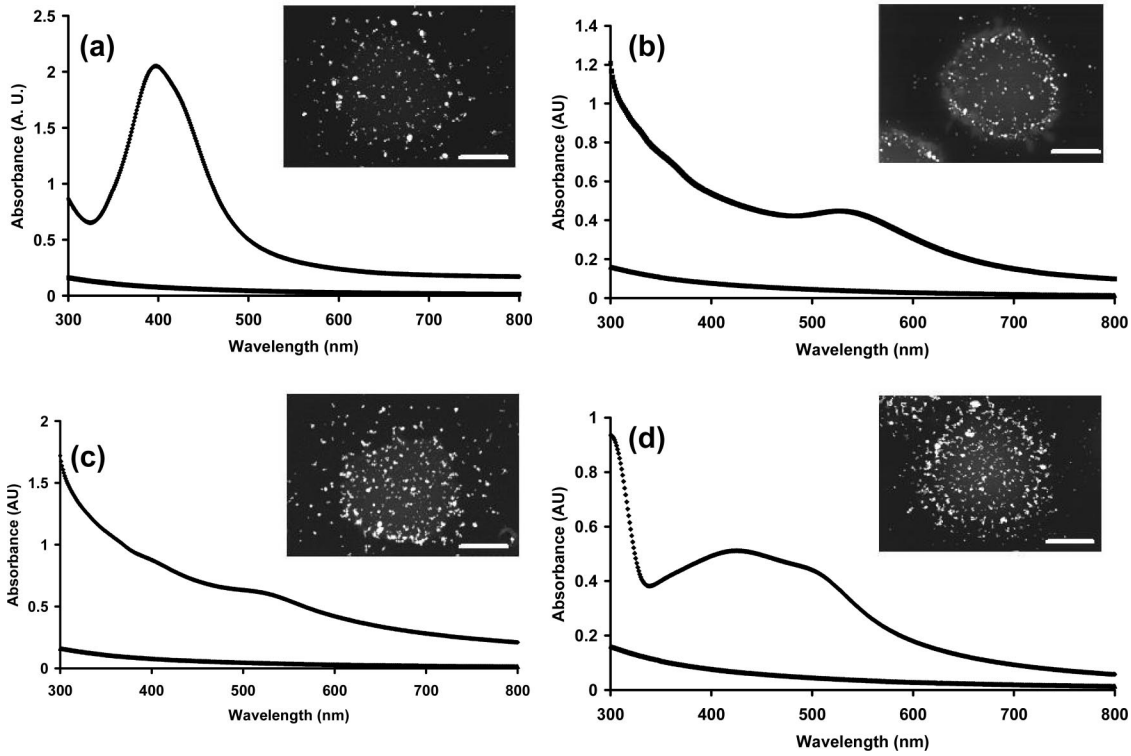


**Figure 5.** Absorbance spectra of the poly(NIPAm-SPP) microgels prior to (bottom spectra) and after template-based NP synthesis (top spectra): (a) monometallic Ag NPs; (b) monometallic Au NPs; (c) bimetallic Ag core-Au shell NPs; (d) bimetallic Au core−Ag shell NPs. Insets show corresponding transmission electron micrographs. Scale bar is 200 nm.

Based on the results shown in Table 1 and Figures 2 −4 we conclude that poly(NIPAm-SPP) microgels showed properties similar to polyelectrolyte microgels. Although the SPP comonomers remained in the charged state, at small concentrations of SPP intermolecular ion coupling was not feasible because the charged groups were not in close proximity to each other, whereas the ionic groups on the same zwitterionic monomer did couple because of restrictions in chain flexibility.[27] Thus in the range of concentrations of SPP studied, the net hydrophilicity of the zwitterionic microgels increased at higher fractions of the ionized SPP comonomer in the polymer network, causing the increase in particle size (Table 1). The results shown in Figures 3 and 4 are consistent with the polyelectrolyte properties of the poly(NIPAm-SPP) microgels. Microgels with a higher concentration of SPP were more hydrophilic and showed higher VPTTs. With increasing salt concentrations, the ionization of the charged groups in the microgels was suppressed and the particles showed lower values of VPTT.

The permanent zwitterionic state of the poly(NIPAm-SPP) microgels and the absence of ion-coupling made these microgels an ideal system for the sequestration of oppositely charged ions, thereby paving the way for the use of these microgels as microreactors for inorganic nanoparticles (NPs).[9,32−34] Furthermore, in contrast with other microgel reactors for inorganic NPs, in the poly(NIPAm-SPP) microgels the oppositely charged groups are in a very close proximity, which can be potentially used for the synthesis of bimetallic NPs.

**Synthesis of Metal NPs in the Interior of Microgels.** In the first step we synthesized silver and gold NPs in the interior of poly(NIPAm-SPP) microgels by sequestering the respective precursor ions, that is, $Ag^+$ or $AuCl_4^-$ ions, and reducing them with $NaBH_4$. Figure 5a shows the UV−vis absorption spectra of the poly(NIPAm-SPP) microgels prior to and after the synthesis of silver NPs. The hybrid microgel showed an absorption peaks at 410 nm, characteristic for silver NPs.[5,35] Figure 5b shows the UV−vis absorption spectra of the poly(NIPAm-SPP) microgels prior to and after the synthesis of gold NPs. Following the synthesis, the microgels showed characteristic absorption peaks at 530 nm, consistent with absorption properties of gold NPs.[36] Inset images a and b in Figure 5 show the representative transmission electron microcopy (TEM) images of hybrid microgels following the synthesis of the silver and gold NPs, respectively. The nanoparticles with dimensions in the range from 8 to 12 nm were localized in the microgel interior.

We used two approaches to the synthesis of bimetallic NPs in the interior of microgels. In the first approach, Ag NPs or Au NPs were synthesized in the microgels, as described above (see panels a and b in Figure 5). In the second stage, $AuCl_4^-$ ions were sequestered into hybrid microgels containing silver NPs, and similarly, $Ag^+$ ions were introduced in the microgels containing gold NPs. Reduction with $NaBH_4$

(32) Zhang, J. G.; Xu, S. Q.; Kumacheva, E. *Adv. Mater.* **2005**, *17*, 2336.
(33) Yang, J. X.; Fang, Y.; Bai, C. L.; Hu, D. D.; Zhang, Y. *Chin. Sci. Bull.* **2004**, *49*, 2026.
(34) Xu, S. Q.; Zhang, J. G.; Paquet, C.; Lin, Y. K.; Kumacheva, E. *Adv. Funct. Mater.* **2003**, *13*, 468.
(35) Mock, J. J.; Barbic, M.; Smith, D. R.; Schultz, D. A.; Schultz, S. *J. Chem. Phys.* **2002**, *116*, 6755.
(36) Jain, P. K.; Lee, K. S.; El-Sayed, I. H.; El-Sayed, M. A. *J. Phys. Chem. B* **2006**, *110*, 7238.

of the ions in the microgel interior was carried out to yield bimetallic NPs. (We note that for hybrid microgels loaded with silver NPs and $AuCl_4^-$ ions, the strong oxidizing properties of the latter enabled the formation of elemental gold on the surface of silver NPs via the redox reaction $3Ag(s) + AuCl_4^- \rightarrow Au(s) + 3Ag^+(aq) + 4\ Cl^-(aq)$ even in the absence of $NaBH_4$.[37])

Figure 5c shows the absorption spectrum of bimetallic Ag−Au NPs synthesized in the microgel template that contained preformed silver NPs. The $AuCl_4^-$ ions could be sequestered at two potential sites, namely, at the surface of silver NPs and at the charged ammonium groups of poly(NIPAm-SPP). The spectrum shows two important features. First, the peak corresponding to the silver NPs (Figure 5a) disappeared, suggesting that the reduced gold coated the surface of Ag NPs, to form a bimetallic core−shell structure.[38] Second, we observed a single peak at 521 nm, slightly blue-shifted in comparison with the plasmonic band of Au NPs (Figure 5b). The energy-dispersive X-ray spectroscopy (EDX) line scans and elemental maps within the resolution of the instrument detected Au and Ag in the same locations. These results suggested the core−shell structure of the NPs.

Figure 5d shows the absorption spectrum of bimetallic Ag−Au NPs synthesized in microgels containing gold NPs. The peak corresponding to the plasmonic band of Au NPs was blue-shifted to 510 nm and that for Ag NPs was red-shifted to 415 nm. This result is consistent with the earlier report on the existence of two characteristic absorbance peaks for core−shell Au−Ag NPs in which one peak increases in absorbance as that component's concentration increases with a corresponding decrease in absorbance in the other peak.[26,39] The EDX line scans, and elemental maps detected Au and Ag in the same locations, within the resolution of the scan. The appearance of two overlapping peaks corresponding to the plasmonic bands of gold and silver NPs indicated that the seed silver NPs were only partially covered with gold. We note that similar to previous reports,[26] in our work, microgels loaded with a mixture of preformed individual Au and Ag NPs showed two well-resolved absorption peaks characteristic for these NPs (not shown).

In the second approach, we synthesized nanoalloy silver−gold particles by co-reduction of $AuCl_4^-$ and $Ag^+$ ions that were simultaneously sequestered into zwitterionic microgels. Figure 6a shows the absorbance spectra of gold−silver NPs prepared in mixtures with $Ag^+/AuCl_4^-$ molar ratios of 3:1, 1:1, and 1:3. The existence of a single, plasmonic band that red-shifted with increasing molar fraction of $AuCl_4^-$ ions suggested the alloy nature of the bimetallic NPs.[34,40] Unlike the spectra obtained for pure Ag NPs (Figure 5a) and pure Au NPs (Figure 5b), the plasmon peaks corresponding to the alloy NPs were broader. Furthermore, the increase in the $Ag^+/AuCl_4^-$ molar ratio was accompanied by a gradual red shift in the wavelength of the plasmonic band, as shown in Figure 6b. The linear dependence of the spectral position of plasmonic band on the ratio of $Ag^+/AuCl_4^-$ was characteristic of alloy NPs,[26] and contrasted with the spectral data reported for core−shell structures that exhibit either two plasmonic bands (when the shell only partially covers the core), or a single peak if the core is completely coated. The intensities of these peaks reflect the respective metal contents.[39,41] The inset Figure 6a shows a TEM image of hybrid microgels containing gold−silver alloy NPs.

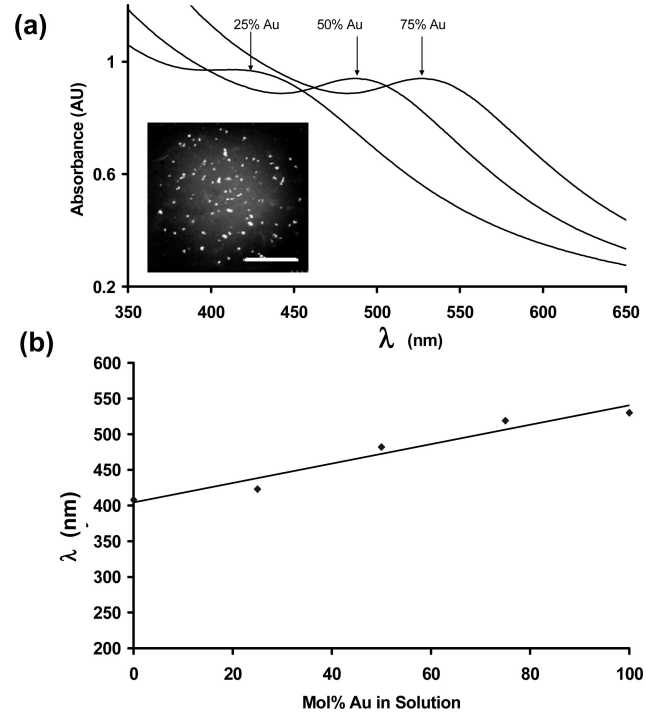


**Figure 6.** (a) UV−vis spectra of Au−Ag alloy NPs synthesized within zwitterionic microgels at in mixtures with $Ag^+/AuCl_4^-$ molar ratios 3:1, 1:1, and 1:3. Inset shows a TEM image of microgels containing Au−Ag alloy NPs synthesized at $Ag^+/AuCl_4^-$ molar ratio of 1:1. Scale bar is 200 nm. (b) Variation in the wavelength of the plasmonic peak of Au/Ag alloy NPs plotted as a function of mole fraction of Au in solution.

We stress that the NPs were synthesized only in the zwitterionic microgels. In the control experiments conducted with the SPP-free microgels (i.e., in the system NS0) we followed the protocol that was used for the NP synthesis in the interior of zwitterionic microgels. No NPs were observed in the SPP-free polyNIPAm microgels, following ion reduction and the purification of the system by centrifugation.

## Conclusion

Zwitterionic PAMs of poly(NIPAm-SPP) can be polymerized only with a limited content of the SPP comonomer because of the propensity of these microgels to aggregation with increasing content of SPP. We found no variation in microgel dimensions with change in pH of the system because of the permanent charge carried by

(37) Lu, X. M.; Tuan, H. Y.; Chen, J. Y.; Li, Z. Y.; Korgel, B. A.; Xia, Y. N. *J. Am. Chem. Soc.* **2007**, *129*, 1733.
(38) Hodak, J. H.; Henglein, A.; Giersig, M.; Hartland, G. V. *J. Phys. Chem. B* **2000**, *104*, 11708.
(39) Mallik, K.; Mandal, M.; Pradhan, N.; Pal, T. *Nano Lett.* **2001**, *1*, 319.
(40) Link, S.; Wang, Z. L.; El-Sayed, M. A. *J. Phys. Chem. B* **1999**, *103*, 3529.
(41) Srnova-Sloufova, I.; Lednicky, F.; Gemperle, A.; Gemperlova, J. *Langmuir* **2000**, *16*, 9928.

the quarternary ammonium and the sulfonate groups. In the range of SPP concentration used in the present work, ion-coupling between the oppositely charged residues is negated by the hydrophilicity imparted to the polymer by the ionized groups. The behavior of zwitterionic microgels in monovalent and divalent salt solutions was found to resemble that of pure polyelectrolytes. Because of the permanent zwitterionic state, the poly(NIPAm-SPP) microgels can be used as efficient sequesters of both anions and cations. In the present work, this feature was exploited for the template-based synthesis of gold, silver, and bimetallic gold−silver alloy and core−shell NPs.

**Acknowledgment.** The authors thank Canada Research Chair fund (NSERC Canada) for financial support of this work.

CM801585X